

In Vivo Imaging of Retinoic Acid Receptor Activity using a Sodium/Iodide Symporter and Luciferase Dual Imaging Reporter Gene

Min Kyung So, Joo Hyun Kang, June-Key Chung, Yong Jin Lee, Jae Hoon Shin, Kwang Il Kim, Jae Min Jeong, Dong Soo Lee, and Myung Chul Lee

Seoul National University College of Medicine

Abstract

Retinoic acids are natural derivatives of vitamin A, and play important roles in modulating tumor cell growth by regulating differentiation, thus suggesting the potential use of these derivatives in cancer therapy and prevention. To visualize the intranuclear responses of functional retinoic acid receptors, we have developed a dual-imaging reporter gene system based on the use of sodium/iodide symporter (NIS) and luciferase in cancer cell lines. NIS and luciferase genes were linked with an internal ribosome entry site, and placed under the control of an artificial *cis*-acting retinoic acid responsive element (pRARE/NL). After retinoic acid treatment, I-125 uptake by pRARE/NL transfected cells was found to have increased by up to about five times that of nontreated cells. The bioluminescence intensity of pRARE/NL transfected cells showed dose-dependency. In vivo luciferase images showed higher intensity in retinoic acid treated SK-RARE/NL tumors, and scintigraphic images of SK-RARE/NL tumors showed increased Tc-99m uptake after retinoic acid treatment. The NIS/luciferase imaging reporter system was sufficiently sensitive to allow the visualization of intranuclear retinoic acid receptor activity. This *cis*-enhancer imaging reporter system may be useful in vitro and in vivo for the evaluation of retinoic acid responses in such areas as cellular differentiation and chemoprevention. *Mol Imaging* (2004) 3, 163–171.

Keywords: retinoic acid receptor, imaging reporter gene, sodium/iodide symporter, luciferase, molecular imaging.

Introduction

Treatment with retinoic acid (RA) can inhibit tumor outgrowth by suppressing cell proliferation, promoting cellular differentiation, or by inducing apoptotic cell death [1]. RAs exert these effects through two main groups of intranuclear receptors belonging to the steroid/thyroid hormone receptor family: retinoic acid receptors (RARs) and retinoid X receptors (RXRs) [2,3]. RARs interact with all-*trans* retinoic acid (ATRA) and 9-*cis* retinoic acid (9-*cis* RA), while RXRs bind 9-*cis* RA [4,5]. Moreover, RXR and RAR, which function as ligand-dependent transcription factors, form heterodimers (RXR/RAR) or homodimers (RXR/RXR) and bind to RA

response elements (RAREs) for modulating the expression of RA response genes in the presence of RAs [6,7].

RAs have been investigated as anticancer and cancer preventive treatments in various clinical trials. Promising results were achieved for acute promyelocytic leukemia (APL), head and neck cancers, and skin neoplasias [8–10]. Clinical trials have shown that RAs are potent tools in various types of cancer, however, many cancers, even of the same origin, do not respond to RA. For example, clinical studies have reported that as many as 60–80% of thyroid cancer patients may not respond to treatment with 13-*cis* RA [11,12]. Also, some types of APL have been reported to be unresponsive to ATRA treatment [13]. For RA therapy, therefore, it is necessary to develop methods of evaluating and predicting treatment response. Some have investigated whether tumors respond to RA by analyzing the mRNAs and protein expression of various receptors in cancer tissues and cell lines [14,15]. However, these methods require tissue samples and cannot be used to evaluate changes in the responses of living subjects.

Recently, molecular imaging using optical, nuclear, and magnetic resonance techniques have been developed to noninvasively, quantitatively, and sequentially visualize and evaluate reporter-gene expression in living animals. In particular, imaging reporter genes have been created by using *cis*-acting reporters to image endogenous gene expression and intracellular signal transduction. Promoters sensitive to a specific intracellular product can be inserted into imaging reporter

Abbreviations: RA, retinoic acid; ATRA, all-*trans* retinoic acid; 9-*cis* RA, 9-*cis* retinoic acid; RAR, retinoic acid receptor; RXR, retinoid receptor; RARE, retinoic acid response element; NIS, sodium/iodide symporter; CCD, charge coupled device; IRES, internal ribosome entry site; CMV, cytomegalovirus; GAPDH, glyceraldehyde-3-phosphate dehydrogenase; PET, positron emission tomography; TSTA, two-step transcriptional amplification.

Corresponding author: June-Key Chung, MD, PhD, Department of Nuclear Medicine, Seoul National University Hospital, 28, Yongon-dong, Chongno-gu, Seoul 110-744, South Korea; e-mail: jkchung@plaza.snu.ac.kr.

Received 19 May 2004; Accepted 7 June 2004.

© 2004 Massachusetts Institute of Technology.

genes. Using this system, several researchers have imaged the activities of estrogen receptor [16], intranuclear factor of activated T cells [17], endogenous p53 gene [18,19], and the cyclooxygenase-2 gene [20].

In this study, we developed a *cis*-imaging reporter system using radionuclide and bioluminescence genes under the control of enhancer regulatory elements that are responsive to RA-specific activators. We also assessed the feasibility of this noninvasive method for visualizing the intranuclear response of RAR to RA treatment *in vitro* and *in vivo*.

Materials and Methods

Retinoic Acid Preparation and Cell Culture Condition

ATRA and 9-*cis* RA were purchased from Sigma (Saint Louis, MO). For *in vitro* treatment, ATRA and 9-*cis* RA were dissolved in absolute ethanol at a concentration of 1 mM. For *in vivo* treatment, ATRA was suspended in 0.2 mL ethanol added to 0.8 mL of corn oil to a concentration of 20 mg/mL, and mixed vigorously to obtain uniform suspensions [21]. These were stored at -20°C , and protected from light.

SK-HEP1 (human hepatocellular carcinoma cell line) was obtained from the Korean Cell Line Bank (KCLB). The cell line was maintained in RPMI-1640 (JBI, Daegu, Korea) containing 10% (vol/vol) FBS, 1% antibiotic-antimycotic containing penicillin, and streptomycin (GIBCO, Grand Island, NY, USA).

Construction of pRARE-NIS/Luciferase Vectors

Human NIS cDNA was kindly provided by Dr. Sissy Jhiang of Ohio State University. NIS and luciferase gene were subcloned into pIRES vector (Clontech, Palo Alto, CA, USA) with a cytomegalovirus (CMV) promoter (pIRES/NL). The CMV promoter, located between the *NdeI* and *NheI* sites, was then removed from the constructed pIRES/NL vector by cutting with the RA restriction enzymes *NdeI* and *NheI* (New England Biolabs, Beverly, MA, USA). The RA enhancer element containing P_{TA} (TA minimal promoter) and TB (transcription blocker) from the plasmid pRARE-TA-SEAP (Clontech) was prepared by PCR using the following primers: forward primer 5'-gggtagcatatggtacgggaggtacttgag-3', and reverse primer 5'-ccactagctagcgtggcgaattcgcgattc-3'. PCR products cut by *NdeI* and *NheI* were then inserted into the plasmid pIRES/NL above (pRARE/NL).

Stable Transfection in SK-HEP1 Cell Line

Transfection was performed using Lipofectamine protocol (Invitrogen, Carlsbad, CA). The pRARE/NL construct was used for stable transfection in the SK-HEP1

cell line. Cells were cultured in media supplemented with 300–800 $\mu\text{g}/\text{mL}$ of geneticin (Invitrogen, Grand Island, NY) to select positive cells. After 14 days, each established clonal line was screened for RA-dependent iodide uptake activity. After RA treatment (1 μM) for 36 hr, the clone with the highest iodide uptake activity was chosen for subsequent studies.

Western Blot Analysis

SK-RARE/NL cells were grown in T-75 dishes and treated with or without ATRA and 9-*cis* RA at 1 μM . Thirty-six hours later, the cells were harvested and lysed with buffer containing 10 mM Tris-HCl (pH 7.5), 1 mM DTT, 20% (vol/vol) glycerol, 1 mM EDTA, and a protease inhibitor mixture. The samples were then centrifuged at 4°C for 5 min and the supernatant was mixed with SDS sample buffer and boiled at 70°C for 10 min. For each sample, 40 μg of protein extract was separated by electrophoresis in a Bis-Tris-HCl buffered 4–12% gradient polyacrylamide gel (Invitrogen, Carlsbad, CA). After proteins had been transferred to nitrocellulose membranes by electroblotting, filters were blocked in 3% skim milk. RARs were detected by incubating the membranes with 1:200 diluted affinity-purified rabbit polyclonal RAR antibodies (Santa Cruz, CA): anti-RAR α (C-20, SC-551), anti-RAR β (C-19, SC-552), and anti-RAR γ (C-19, SC-550). α -Tubulin was detected with α -tubulin antibody (Clone B-5-1-2; Sigma; dilution, 1:1000). After washing, membranes were incubated with their respective secondary antibody for 1.5 hr. Immunoreactive bands were detected by chemiluminescence ECL (Roche, Mannheim, Germany).

In Vitro Radioiodide Uptake Assay

SK-RARE/NL and wild-type SK-HEP1 cells were plated at a cell density of 1×10^5 in 24-well plates with serum-containing RPMI-1640 medium. 1 mM of RA was added at selected intervals. Additionally, several doses of RA were evaluated for 36 hr. After incubation with RA, I-125 uptake levels were determined. Iodide uptake assays were performed using a modification of the method described by Weiss et al. [22]. Briefly, 24-well plates were aspirated, and then iodide uptake levels were determined by exposing the cells at 37°C for 30 min to 0.5 mL Hanks balanced salt solution (HBSS) containing 0.5% bovine serum albumin, 10 mM 2-[4-(2-hydroxyethyl)-1-piperziny]ethanesulfonic acid-NaOH (pH 7.3), 10 μM NaI, and carrier-free Na[I-125] with a specific activity of 3.7 kBq (0.1 μCi). Some reactions were performed in this assay buffer supplemented with the NIS inhibitor NaClO_4 at 30 μM to control for specific uptake. The cells were then washed twice rapidly (<15 sec) with 2 mL

of iodide-free ice-cold HBSS buffer, detached with 0.2% SDS, and radioactivity was measured using a gamma counter (Cobra II, Canberra Packard, USA). Protein concentrations in cell homogenates were determined by using a modified Bradford protein assay (Bio-Rad, Munich, Germany). Results are expressed as the amount of iodide accumulated per protein amount.

In Vitro Bioluminescence Assay

Cell lines were plated and treated with RA as described above. Later, RA was washed from each well using PBS, and bioluminescence assays were performed using a Luciferase Assay Kit (Applied Biosystem, Bedford, MA, USA). Lysis solution was then added to each well, and cells were detached from the plates. Cell lysates from each well were then transferred to a microplate and bioluminescence was measured using a microplate luminometer (TR717; Applied Biosystem).

RT-PCR Analysis

Cells were harvested by scraping, and total RNA was isolated using TRIZOL Reagent (Invitrogen, Carlsbad, CA) according to the manufacturer's instructions with slight modification. Briefly, 400 ng of total RNA was reverse transcribed in a final volume of 20 μ L containing 1 μ L Oligo (dT), 4 μ L $5 \times$ first strand buffer, 2 μ L 0.1 M DTT, 1 μ L 10 mM dNTP mix, and M-MLV reverse transcriptase (Invitrogen, Grand Island, NY). The following PCR was then performed for confirming NIS and luciferase mRNA expressions with a total volume of 20 μ L containing 2 μ L of the cDNA, 2 μ L of $10 \times$ reaction buffer, forward primer, and reverse primer; 1 μ L of 10 mM dNTP mix; and 2.5 units of Tag-DNA polymerase (Gene-Draft, Munster, Germany). The primer sequences and the reaction profiles used were as follows: NIS, 5'-gtcggaggcctatcgcta-3' (forward), 5'-gccgtgtagaagggtcagat-3' (reverse), and an initial denaturation at 95°C for 10 min; elongation for 25 cycles at 95°C for 15 sec, 50°C for 30 sec, and 73°C for 30 sec; followed by a final extension at 73°C for 7 min. Luciferase PCR was performed using: 5'-cgccttgattgacaaggatgg-3, 5'-ggccttatgagatctctct-3'; an initial denaturation at 94°C for 10 min; 25 cycles of elongation at 94°C for 45 sec, 53°C for 30 sec, and 72°C for 1 min; and a final extension at 72°C for 7 min. Glyceraldehyde-3-phosphate dehydrogenase (GAPDH) PCR was performed using: 5'-accagggtctgttttaactct-3', 5'-gagtccttcacgataccaaag-3'; an initial denaturation at 94°C for 10 min; 25 cycles of elongation at 94°C for 30 sec, 57°C for 30 sec, and 72°C for 30 sec; and a final extension at 72°C for 7 min. All PCR products were analyzed by ethidium bromide-stained agarose gel electrophoresis.

Generation of Tumor Xenografts in Nude Mice

The animal study was conducted with the approval of the Seoul National University Animal Research Committee, and according to the guidelines for the care and use of laboratory animals. For bioluminescence imaging, six male BALB/c nude mice received a subcutaneous flank injection containing different numbers of cells suspended in 100 μ L of RPMI-1640 medium as follows: left shoulder (SK-Hep1; 8×10^6), right shoulder (SK-RARE/NL; 1×10^6), left leg (SK-RARE/NL; 4×10^6), and right leg (SK-RARE/NL; 8×10^6). After allowing 3 days for tumor growth, bioluminescence images were acquired.

To obtain gamma camera images, SK-HEP1 and SK-RARE/NL cells were implanted in three nude mice: left shoulder (SK-Hep1; 1×10^7), right shoulder (SK-RARE/NL; 1×10^6), left leg (SK-RARE/NL; 1×10^7), and right leg (SK-RARE/NL; 1×10^8). Tumors were allowed to grow, and became established in 3 weeks. Gamma camera images were obtained when the tumor size in the right leg reached a diameter of 0.7–1.3 cm; sites injected with fewer cells produced smaller diameter tumors.

In Vivo Bioluminescence and Gamma Camera Images

For optical image acquisition, an aqueous solution of the luciferase substrate luciferin (5 mg/mice; Molecular Probes, Palo Alto, CA, USA) was mixed with 300 μ L of an anesthetic composed of ketamine (50 mg/ μ L), rompun (23.32 mg/ μ L), and saline solution (2:1:18). This solution was injected into the peritoneal cavity 10 min before imaging. Test animals were placed individually in the LAS-3000 equipped with a cooled CCD camera (Fuji Film, Tokyo, Japan). After gray-scale images under white light were captured, bioluminescent images were acquired by collecting and integrating the light for 20 min. Rainbow scale pseudocolor images were converted and superimposed over gray-scale images and processed using graphic software (Photoshop 6.0, Adobe, San Jose, CA, USA).

To obtain gamma camera images, 1 hr after injecting 11.1 MBq (300 μ Ci) of Tc-99m into the peritoneal cavity, mice with tumors were placed in a spread-prone position, and scanned with a gamma camera (ON 410; Ohio Nuclear, Solon, OH, USA) equipped with a pinhole collimator. The acquired gamma camera images were quantified using the Multigauge Image-Analysis Program (Fuji Film).

To demonstrate the dose-dependent induction of luciferase gene expression in vivo, at each RA concentration two control mice were not treated with ATRA, while the other mice received 100 or 200 mg/kg body weight doses of ATRA orally. Mice were imaged with a CCD camera 48 hr after ATRA administration. To

demonstrate the time-dependent induction of luciferase and NIS gene expression in vivo, 1 day after obtaining the images of mice not treated with RA, animals were orally administered ATRA, 100 (for luciferase imaging) or 200 (for NIS imaging) mg/kg body weight. Bioluminescence and gamma camera images of nude mice were obtained as described above 24 or 48 hr after ATRA administration.

Results

pRARE/NL Construction

We constructed a reporter gene with an artificial promoter containing two copies of the RARE enhancer element and a minimal TA promoter. We developed a dual-modality reporter imaging system based on the NIS and luciferase genes, which were *cis*-linked to the reporter gene by an IRES sequence.

Protein Expressions of RAR α , RAR β , and RAR γ in SK-HEP1 Cell Line

SK-HEP1 expressed the nuclear RA receptors RAR α , RAR β , RAR γ . Immunoreactive bands for RAR α , RAR β , and RAR γ were detected in SK-HEP1 total protein samples with or without RA treatment, as shown in Figure 1.

In Vitro Iodide Uptake and Bioluminescence Assay to Monitor NIS and Luciferase Expression According to Response RAs

In SK-RARE/NL cells, radioiodide uptake and bioluminescence activity were significantly increased after adding 1 μ M of ATRA at 12 hr, and peaked at 36 hr.

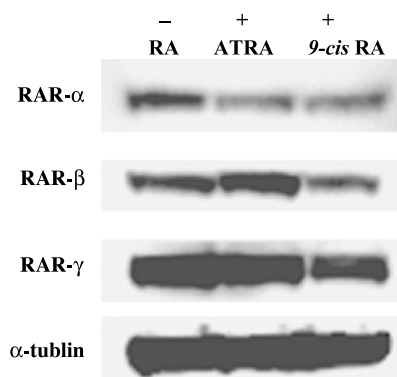


Figure 1. Expression profile of retinoic acid receptors in SK-HEP1 cells. Western blotting was performed with total protein from SK-HEP1 cells treated with or without 1 μ M ATRA or 9-*cis* RA for 36 hours. SK-HEP1 cell lysates were prepared and subjected to a Bis-Tris-HCl buffered 4–12% gradient polyacrylamide gel (40 μ g protein/lane), and electroblotted onto nitrocellulose membranes. Immunochemical detection was carried out with anti-RAR α (C-20), anti-RAR β (C-19), anti-RAR γ (C-19) and anti- α -tubulin, and a chemiluminescence ECL kit.

9-*cis* RA treatment also induced iodide uptake and bioluminescence activity in the same manner as ATRA (Figure 2).

Faint NIS and luciferase PCR products were detected by RT-PCR analysis prior to RA treatment in SK-RARE/NL cells (Figure 3, lane 0 hr). Both ATRA and 9-*cis* RA stimulated an increase in NIS and luciferase mRNA products. NIS and luciferase expression patterns due to 9-*cis* RA treatment were similar to those of ATRA treatment (Figure 3).

The levels of NIS and luciferase activity in SK-RARE/NL cells treated with ATRA increased in a dose-dependent manner (Figure 4). Iodide uptake was completely blocked by 30 μ M potassium perchlorate (KClO₄), a specific inhibitor of NIS. These results were compared with those of nontransfected SK-HEP1 as a negative control. SK-HEP1 cells concentrated only a small amount of I-125 at baseline and exhibited negligible bioluminescent activity. The NIS and luciferase activity of SK-RARE/NL treated with ATRA was considerably high compared to that of SK-HEP1. These high baseline expressions of NIS and luciferase in SK-RARE/NL may be due to retinoid or retinoid-related compounds in culture medium. No difference in NIS or luciferase activity was observed between SK-HEP1 RA-treated or nontreated cells (insets in Figure 4A and B). Maximally induced levels of radioiodide uptake and bioluminescence activity in ATRA-treated transfected SK-RARE/NL were compared with levels in SK-HEP1 cells, and found to be greater by 50-fold and 550-fold, respectively. SK-RARE/NL showed 5-fold and 2.5-fold increases in iodide uptake and bioluminescence activity versus unstimulated cells, respectively. A good correlation ($r^2 = .937$) was obtained between iodide uptake and bioluminescence activity at all RA doses tested (Figure 4C). Similar correlations were seen in pRARE/NL transfected HEK-293 cells (data not shown).

Monitoring Retinoic Acid Receptor Activity by Scintigraphic Imaging In Vivo

Before ATRA administration, gamma camera images of mice revealed minimal uptake of Tc-99m in SK-HEP1 xenografts, whereas SK-RARE/NL xenografts tumors showed faint uptake (Figure 5A, left panel). Twenty-four hours after systemic ATRA administration (4 mg/kg), elevated Tc-99m uptake was observed (Figure 5A, middle panel). At 48 hr, increased Tc-99m uptake was observed in SK-RARE/NL xenografts, especially in the right leg tumors versus wild-type SK-HEP1 xenografts and nontreated SK-RARE/NL xenografts (Figure 5A, right panel). The quantitative analysis of gamma camera images demonstrated that NIS expression was similar pre- and post-ATRA treatment in SK-HEP1 tumors, but there

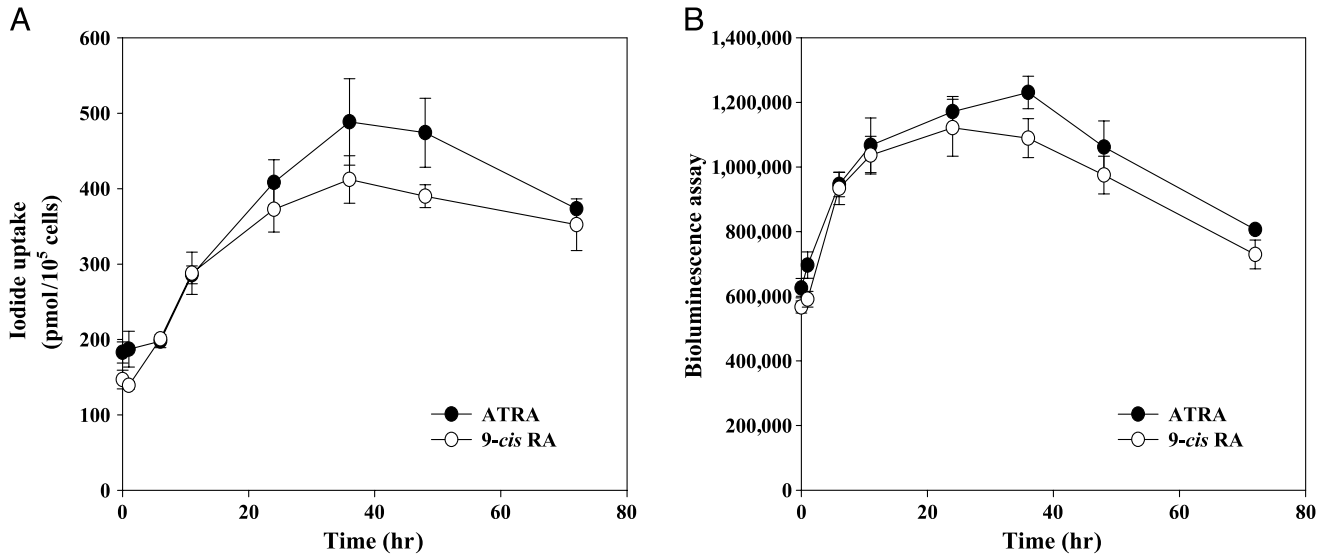


Figure 2. Time course of the RA-induced up-regulation of NIS and luciferase activity. After inoculating 1×10^5 of SK-RARE/NL in 24-plate well, cells were treated with $1 \mu\text{M}$ ATRA or 9-cis RA for the indicated times, and then radioiodide accumulation (A) and luciferase activity (B) were measured. (●) SK-RARE/NL with ATRA treatment; (○), SK-RARE/NL with 9-cis RA treatment. Values are expressed as means \pm SD ($n = 3$).

was increased Tc-99m accumulation in ATRA-treated SK-RARE/NL tumors versus the non-ATRA-treated group ($n = 3$, Figure 5B).

Optical Bioluminescence Imaging of RA Activity In Vivo

Bioluminescence images demonstrated that ATRA-treated mice with SK-RARE/NL tumors had higher bioluminescence intensity than nontreated mice, whereas no bioluminescence signal was observed in SK-HEP1 tumors (the shoulder) regardless of ATRA treatment (Figure 6).

We observed the time-dependent induction of luciferase gene expression from the RARE promoter in same mice. No signal was observed in SK-HEP1 tumors regardless of RA treatment. In contrast, baseline luciferase expression in nonstimulated pRARE-NL construct-bearing mice was only faintly detected (Figure 7, left mouse).

Twenty-four hours after systemic ATRA administration to these mice, elevated luciferase expression was observed (Figure 7, middle mouse). At 48 hr, bioluminescence images of SK-RARE/NL tumors showed higher intensity in mice treated with RA than in the control mouse (Figure 7, right mouse). Ninety-six hours after RA administration, mice showed substantially less luciferase activity in pRARE/NL-bearing tumors (data not shown).

Discussion

Many studies have shown in experimental animal models that RA can reduce tumor growth rates and size in thyroid, breast, leukemia, head and neck cancers, and therefore suggest that RA could be used for cancer therapy [9,23–26]. RAs act through intranuclear RA receptors that ultimately activate target genes. RA target

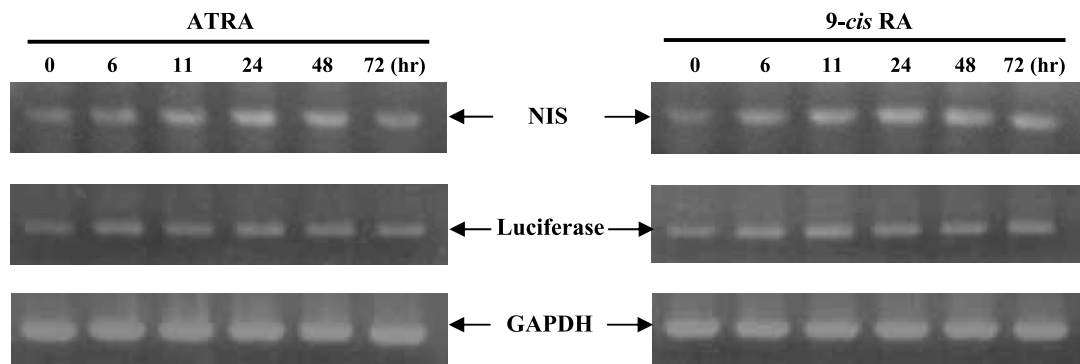


Figure 3. Expression of NIS and luciferase mRNA in RA treated SK-RARE/NL cells. SK-RARE/NL cells were treated with $1 \mu\text{M}$ ATRA or 9-cis RA for the indicated times and then RT-PCR was performed on total RNA. GAPDH was used as an internal control.

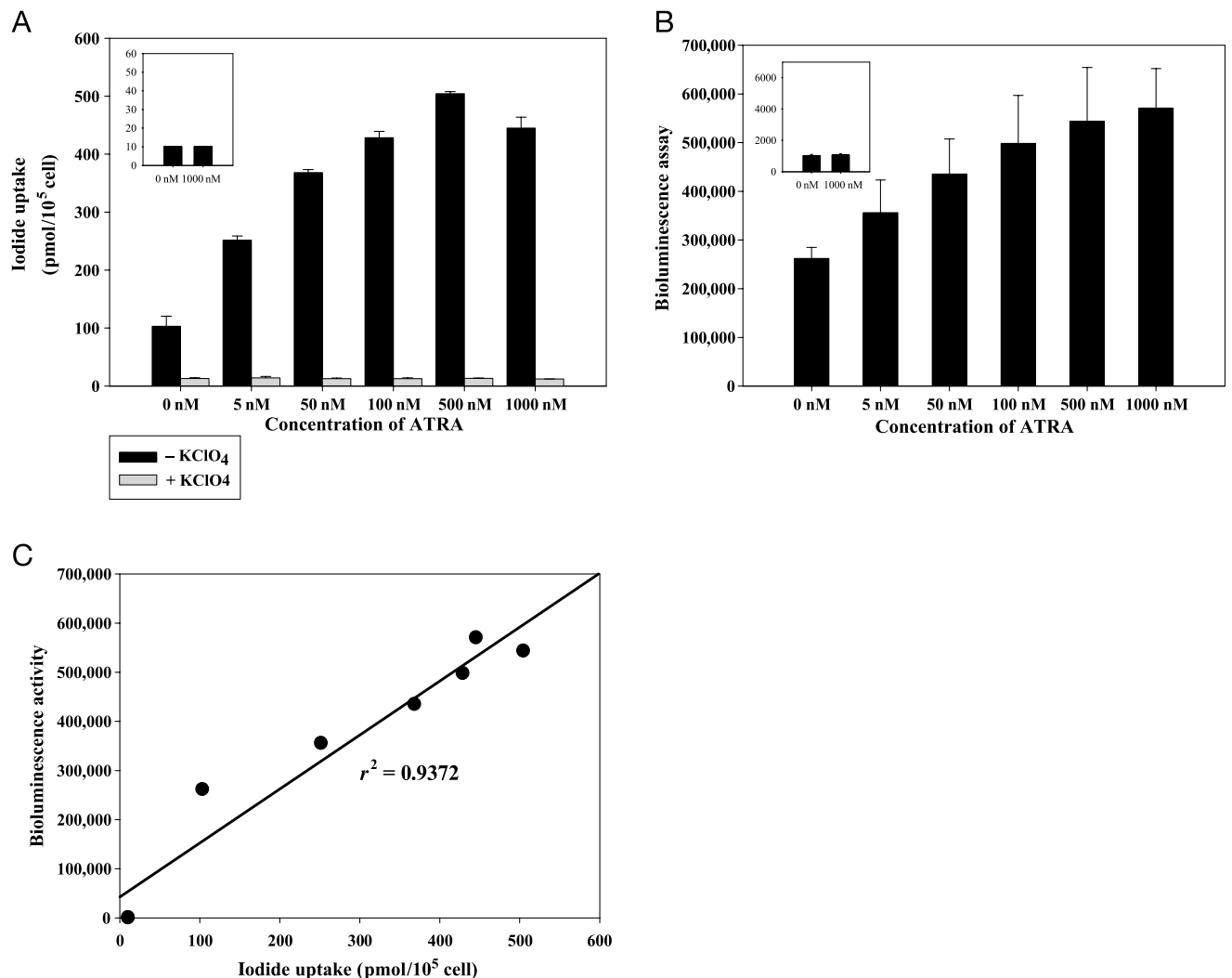


Figure 4. *In vitro* radioiodide uptake assay and bioluminescence assay according to the dose dependency of ATRA. After inoculating 1×10^5 of SK-RARE/NL or SK-HEP1 (control cells) into 24-well plates, each well was treated with different doses of ATRA. Thirty-six hours after treatment, radioiodide uptake (A) and bioluminescence (B) assays were performed *in vitro*. The figures inserted in (A) and (B) indicate SK-HEP1 cell line with or without ATRA treatment. (C) Linear regression analysis showed a correlation between I-125 uptake and bioluminescence activity at various ATRA concentrations.

genes contain RARE in their promoters, and their expression is directly regulated by RA [6]. In experiments performed in clinical settings, resistance to the actions of RA has often been encountered [13,27–29]. The causes of this resistance are not completely understood, but are thought to be associated with mutations in the ligand-binding domain of RAR [27]. Decreased RAR β expression has also been observed in patients with breast carcinoma and in patients with premalignant oral lesions [30–33]. Due to these findings, before RA treatment is adopted, it is necessary to confirm whether or not the patient is responsive.

For the purposes of analyzing RA effects in living subjects, we developed a *cis*-reporting imaging methodology based on optical and nuclear reporter systems to visualize the activity of RAR *in vitro* and *in vivo*. Optical

reporter systems, such as bioluminescence and fluorescence modalities, are both cost- and time-efficient, require less resource and space than more conventional imaging methods such as positron emission tomography (PET), and are particularly well suited for imaging small animals. Optical reporter systems have also been shown to be very useful and cost-effective *in vitro* assays for validating the function and sensitivity of specific inducible reporter systems. Nevertheless, optical imaging techniques do not provide tomographic images or quantitative information, and are difficult to translate into human use. In addition, their other major limitations include light scattering and insufficient depth penetration. Thus, this method is restricted to small research animals like mice and rats, or to superficial tissue sites in larger animals [34,35].

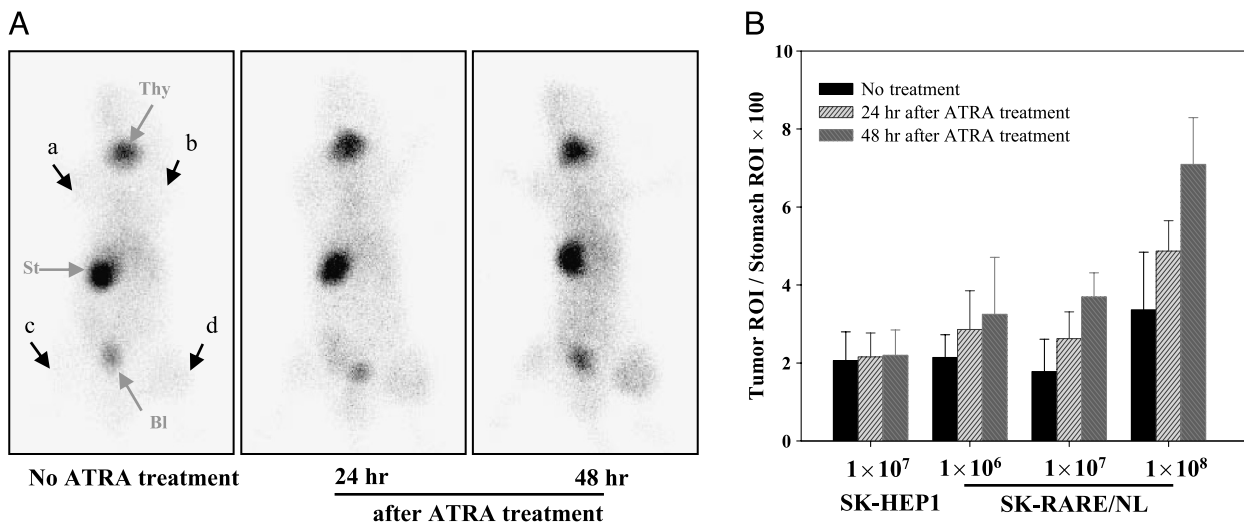


Figure 5. Noninvasive and repetitive Tc-99m accumulation imaging by NIS according to the response of RA in nude mice bearing SK-HEP1 and SK-RARE/NL tumors. Xenograft tumors derived from SK-HEP1 and SK-RARE/NL cells were grown in male nude mice by subcutaneous injection (a, 1 × 10⁷ wild-type SK-HEP1 cells; b, 1 × 10⁶ SK-RARE/NL cells; c, 1 × 10⁷ SK-RARE/NL cells; d, 1 × 10⁸ SK-RARE/NL cells). Three weeks after cell injection, each mouse was injected intraperitoneally with 11.1 MBq (300 μCi) of Tc-99m. Animals were treated with 200 mg/kg ATRA by oral administration. (A) Serial planar gamma camera images of nude mice bearing SK-HEP1 and SK-RARE/NL tumors before ATRA treatment and 24 or 48 hr after treatment were taken. All images are from representative mice (Thy = thyroid; St = stomach; Bl = bladder). (B) Intensity ratio of each tumor in mice before and after treatment of ATRA. Data were normalized versus the stomach region of interest (ROI). Values are mean ± SD (n = 3).

Nuclear-based reporter systems using PET and the gamma camera are more easily applied to larger subjects, and they provide the opportunity to obtain tomographies and to quantitatively measure reporter gene expression [34,36,37]. Originally, PET-based imaging reporter systems, such as herpes virus 1 thymidine kinase (HSV1-tk) [38] and dopamine receptor type

2 (hD₂R) [39], were utilized. These PET reporter techniques have limitations, as they require the synthesis of complicated substrates and the use of expensive equipment, and have some physiologic effects on normal cellular function. NIS also has many advantages as an imaging reporter gene compared to PET [40,41]. NIS uses a wide availability of substrates such as radioiodines

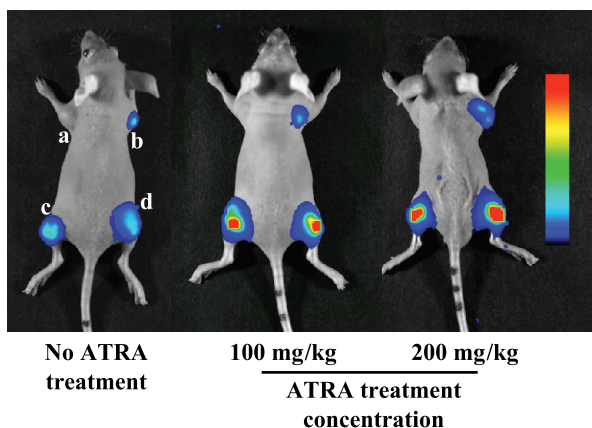


Figure 6. Bioluminescence imaging of dose-dependent luciferase expression using the cis-acting promoter system. Xenograft tumors derived from SK-HEP1 and SK-RARE/NL cells were grown in male nude mice by subcutaneous injection (a, 8 × 10⁶ wild type SK-HEP1 cells; b, 1 × 10⁶ SK-RARE/NL cells; c, 4 × 10⁶ SK-RARE/NL cells; d, 8 × 10⁶ SK-RARE/NL cells). Three days after cell injection, ATRA was administered orally at 0, 100 or 200 mg/kg to two mice. Forty-eight hours after administration, bioluminescence imaging was performed with a CCD camera. Mice were anesthetized, and injected intraperitoneally with luciferin (5 mg/mouse), and then imaged for in vivo dose-dependent luciferase expression assay.

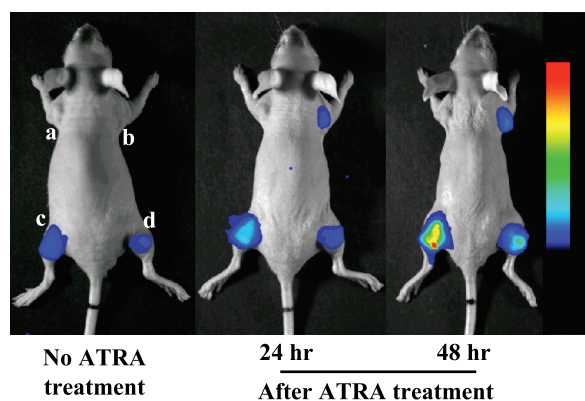


Figure 7. Noninvasive and repetitive bioluminescence imaging by luciferase activity according to RA response in vivo. Xenograft tumors derived from SK-HEP1 and SK-RARE/NL cells were grown in three male nude mice by subcutaneous injection (a, 8 × 10⁶ wild-type SK-HEP1 cells; b, 1 × 10⁶ SK-RARE/NL cells; c, 4 × 10⁶ SK-RARE/NL cells; d, 8 × 10⁶ SK-RARE/NL cells). Three days after injection, mice were imaged at 20 min after intraperitoneal injection of luciferin (5 mg/mouse). Mice were treated with 200 mg/kg ATRA orally. At 24 hours and again 48 hours after ATRA administration, mice were again anesthetized, and injected intraperitoneally with luciferin, and imaged for time-dependent luciferase expression. All images were obtained from a single representative mouse.

and Tc-99m, which are simpler in structure to those used in PET scanning, and the metabolism and clearance of these substrates in the body is well understood. It is cost-effective and there is no problem of labeling stability when using radioiodines or Tc-99m.

To overcome the shortcomings inherent in using either a NIS or luciferase modality, we created a superior system by linking the NIS reporter and luciferase reporter via an IRES [42]. Such a dual-reporter system overcomes the weaknesses of each modality by combining their strengths. Using this system, the activity of intranuclear RAR can be visualized using luminescent and scintigraphic images, and therefore eases the transition from animal experimentation to the clinical trial stage.

In this study, the *cis*-enhancer system RARE was constructed to be induced and regulated by specific endogenous transcription factors (RA-bound RAR). The upstream promoter of the *cis*-enhancer system is weak compared to a constitutive promoter such as the CMV promoter. Optical bioluminescence has high sensitivity and allows for the clear visualization of luciferase expression, which is under the control of a weak promoter. But NIS imaging, which requires higher levels of reporter gene expression and/or higher numbers of expressing cells, was less effective at imaging.

Our result showed considerable background activity and the fold increase of reporter pair was somewhat low. It is possible that endogenous serum retinoid will activate reporter expression in cell culture and animal models to produce background expression.

For improved NIS image acquisition, it was essential to enhance the transcriptional activity of the RA-targeted promoter. To accomplish this, we needed to apply an amplification approach such as a two-step transcriptional amplification (TSTA). In the TSTA system, a potent transcriptional activator acts on a second expression plasmid encoding the reporter/therapeutic protein. This two-step approach results in the cell-specific amplification of gene expression [43,44]. The approaches validated by the present study should lead to better vectors with the RARE promoter to facilitate detection of specific responses in vivo. Huang et al. [45] reported the increased radioiodine uptake and retention by the combination to NIS and thyroperoxidase (TPO) gene expression. To obtain the enhanced NIS image, coexpression of TPO gene will be helpful.

The induction of NIS and luciferase expression in xenograft mice models required a relatively large dose of ATRA. The dose necessary for maximum reporter gene induction was 10- to 20-fold, the maximum tolerable dose for human patients with solid tumors [46,47]. No

significant signs of RA toxicity, such as skin scaling or weight loss, were observed in mice after a single oral ATRA dose of 100 mg/kg; however, at 200 mg/kg weight loss and skin scaling were evident. TSTA may allow the ATRA dose to be reduced.

In conclusion, we visualized and evaluated the function of RAR using scintigraphic and bioluminescent optical images in living mice. The establishment of this method may open an avenue to new therapeutic approaches based on the measurement of RA's effectiveness and allow for more detailed analysis of its use in cancer treatment.

Acknowledgments

This study was supported by a grant of the National Cancer Control R&D Program 2004, Ministry of Health and Welfare, Republic of Korea, and MK So, JH Kang, J-K Chung, YJ Lee, JH Shin were supported by the BK21 project for Medicine, Dentistry, and Pharmacy (2004).

References

- [1] Merino R, Hurler JM (2003). The molecular basis of retinoid action in tumors. *Trends Mol Med.* **9**:509–511.
- [2] Giguere V, Evans RM (1990). Identification of receptors for retinoids as members of the steroid and thyroid hormone receptor family. *Methods Enzymol.* **189**:223–232.
- [3] Zusi FC, Lorenzi MV, Vivat-Hannah V (2002). Selective retinoids and rexinoids in cancer therapy and chemoprevention. *Drug Discov Today.* **7**:1165–1174.
- [4] Levin AA, Sturzenbecker LJ, Kazmer S, Bosakowski T, Huselton C, Allenby G, Speck J, Kratzenstein C, Rosenberger M, Lovey A, Grippo JF (1992). 9-cis retinoic acid stereoisomer binds and activates the nuclear receptor RXR alpha. *Nature.* **355**:359–361.
- [5] Allenby G, Bocquel MT, Saunders M, Kazmer S, Speck J, Rosenberger M, Lovey A, Kastner P, Grippo JF, Chambon P, Levin AA (1993). Retinoic acid receptors and retinoid X receptors: interactions with endogenous retinoic acids. *Proc Natl Acad Sci USA.* **90**:30–34.
- [6] Wei LN (2003). Retinoid receptors and their coregulators. *Annu Rev Pharmacol Toxicol.* **43**:47–72.
- [7] Egea PF, Rochel N, Birck C, Vachette P, Timmins PA, Moras D (2001). Effects of ligand binding on the association properties and conformation in solution of retinoic acid receptors RXR and RAR. *J Mol Biol.* **307**:557–576.
- [8] Castaigne S, Chomienne C, Daniel MT, Ballerini P, Berger R, Fenau P, Degos L (1990). All-trans retinoic acid as a differentiation therapy for acute promyelocytic leukemia: I. Clinical results. *Blood.* **76**:1704–1709.
- [9] Huber MH, Hong WK (1994). Biology and chemoprevention of head and neck cancer. *Curr Probl Cancer.* **18**:81–140.
- [10] Verma AK (1987). Inhibition of both stage I and stage II mouse skin tumour promotion by retinoic acid and the dependence of inhibition of tumor promotion on the duration of retinoic acid treatment. *Cancer Res.* **47**:5097–5101.
- [11] Haugen BR, Larson LL, Pugazhenthii U, Hays WR, Klopper JP, Kramer CA, Sharma V (2004). Retinoic acid and retinoid X receptors are differentially expressed in thyroid cancer and thyroid carcinoma cell lines and predict response to treatment with retinoids. *J Clin Endocrinol Metab.* **89**:272–280.

- [12] Schmutzler C, Kohrle J (2000). Retinoic acid redifferentiation therapy for thyroid cancer. *Thyroid*. **10**:393–406.
- [13] Gallagher RE (2002). Retinoic acid resistance in acute promyelocytic leukemia. *Leukemia*. **16**:1940–1958.
- [14] Burnett AK, Grimwade D, Solomon E, Wheatley K, Goldstone AH (1999). Presenting white blood cell count and kinetics of molecular remission predict prognosis in acute promyelocytic leukemia treated with all-trans retinoic acid: Result of the Randomized MRC Trial. *Blood*. **93**:4131–4143.
- [15] Xu XC, Ro JY, Lee JS, Shin DM, Hong WK, Lotan R (1994). Differential expression of nuclear retinoid receptors in normal, premalignant, and malignant head and neck tissues. *Cancer Res*. **54**:3580–3587.
- [16] Ciana P, Raviscioni M, Mussi P, Vegeto E, Que I, Parker MG, Lowik C, Maggi A (2003). In vivo imaging of transcriptionally active estrogen receptors. *Nat Med*. **9**:82–86.
- [17] Ponomarev V, Doubrovin M, Lyddane C, Beresten T, Balatoni J, Bornman W, Finn R, Akhurst T, Larson S, Blasberg R, Sadelain M, Tjuvajev JG (2001). Imaging TCR-dependent NFAT-mediated T-cell activation with positron emission tomography in vivo. *Neoplasia*. **3**:480–488.
- [18] Doubrovin M, Ponomarev V, Beresten T, Balatoni J, Bornmann W, Finn R, Humm J, Larson S, Sadelain M, Blasberg R, Tjuvajev JG (2001). Imaging transcriptional regulation of p53-dependent genes with positron emission tomography in vivo. *Proc Natl Acad Sci USA*. **98**:9300–9305.
- [19] Wang W, El-Deiry WS (2003). Bioluminescent molecular imaging of endogenous and exogenous p53-mediated transcription in vitro and in vivo using an HCT116 human colon carcinoma xenograft model. *Cancer Biol Ther*. **2**:196–202.
- [20] Nguyen JT, Machado H, Herschman HR (2003). Repetitive, noninvasive imaging of cyclooxygenase-2 gene expression in living mice. *Mol Imaging Biol*. **5**:248–256.
- [21] Nugent P, Pisano MM, Weinrich MC, Greene RM (2002). Increased susceptibility to retinoid-induced teratogenesis in TGF-beta2 knockout mice. *Reprod Toxicol*. **16**:741–747.
- [22] Weiss SJ, Philp NJ, Grollman EF (1984). Iodide transport in a continuous line of cultured cells from rat thyroid. *Endocrinology*. **114**:1090–1098.
- [23] Bollag W, Holdener EE (1992). Retinoids in cancer prevention and therapy. *Ann Oncol*. **3**:513–526.
- [24] Tallman MS, Wiernik PH (1992). Retinoids in cancer treatment. *J Clin Pharmacol*. **32**:868–888.
- [25] Moon RC, Mehta RG (1989). Chemoprevention of experimental carcinogenesis in animals. *Prev Med*. **18**:576–591.
- [26] Simon D, Koehle J, Reiners C, Boerner AR, Schmutzler C, Mainz K, Goretzki PE, Roeher HD (1998). Redifferentiation therapy with retinoids: Therapeutic option for advanced follicular and papillary thyroid carcinoma. *World J Surg*. **22**:569–574.
- [27] Krut FA, van der Veer LJ, Mader S, van den Brink CE, Feijen A, Jonk IJ, Kruijer W, van der Saag PT (1992). Retinoic acid resistance of the variant embryonal carcinoma cell line RAC65 is caused by expression of a truncated RAR alpha. *Differentiation*. **49**:27–37.
- [28] Tari AM, Lim SJ, Hung MC, Esteva FJ, Lopez-Berestein G (2002). Her2/neu induces all-trans retinoic acid (ATRA) resistance in breast cancer cells. *Oncogene*. **21**:5224–5232.
- [29] Geradts J, Chen JY, Russell EK, Yankaskas JR, Nieves L, Minna JD (1993). Human lung cancer cell lines exhibit resistance to retinoic acid treatment. *Cell Growth Differ*. **4**:799–809.
- [30] Xu XC, Sneige N, Liu X, Nandagiri R, Lee JJ, Lukmanji F, Hortobagyi G, Lippman SM, Dhingra K, Lotan R (1997). Progressive decrease in nuclear retinoic acid receptor beta messenger RNA level during breast carcinogenesis. *Cancer Res*. **57**:4992–4996.
- [31] Lotan R, Xu XC, Lippman SM, Ro JY, Lee JS, Lee JJ, Hong WK (1995). Suppression of retinoic acid receptor-beta in premalignant oral lesions and its up-regulation by isotretinoin. *N Engl J Med*. **332**:1405–1410.
- [32] Roman SD, Clarke CL, Hall RE, Alexander IE, Sutherland RL (1992). Expression and regulation of retinoic acid receptors in human breast cancer cells. *Cancer Res*. **52**:2236–2242.
- [33] Zhang XK, Liu Y, Lee MO (1996). Retinoid receptors in human lung cancer and breast cancer. *Mutat Res*. **350**:267–277.
- [34] Contag PR (2002). Whole-animal cellular and molecular imaging to accelerate drug development. *Drug Discov Today*. **7**:555–562.
- [35] Edinger M, Hoffmann P, Contag CH, Negrin RS (2003). Evaluation of effector cell fate and function by in vivo bioluminescence imaging. *Methods*. **31**:172–179.
- [36] Blasberg RG, Gelovani J (2002). Molecular-genetic imaging: A nuclear medicine-based perspective. *Mol Imaging*. **1**:280–300.
- [37] Gambhir SS (2002). Molecular imaging of cancer with positron emission tomography. *Nat Rev Cancer*. **2**:683–693.
- [38] Tjuvajev JG, Finn R, Watanabe K, Joshi R, Oku T, Kennedy J, Beattie B, Koutcher J, Larson S, Blasberg RG (1996). Noninvasive imaging of herpes virus thymidine kinase gene transfer and expression: A potential method for monitoring clinical gene therapy. *Cancer Res*. **56**:4087–4095.
- [39] Liang Q, Satyamurthy N, Barrio JR, Toyokuni T, Phelps MP, Gambhir SS, Herschman HR (2001). Noninvasive, quantitative imaging in living animals of a mutant dopamine D2 receptor reporter gene in which ligand binding is uncoupled from signal transduction. *Gene Ther*. **8**:1490–1498.
- [40] Chung JK (2002). Sodium iodide symporter: Its role in nuclear medicine. *J Nucl Med*. **43**:1188–1200.
- [41] Chung JK, Kang JH (2004). Translational research using the sodium/iodide symporter in imaging and therapy. *Eur J Nucl Med Mol Imaging*. **31**:799–802.
- [42] Pelletier J, Sonenberg N (1988). Internal initiation of translation of eukaryotic mRNA directed by a sequence derived from poliovirus RNA. *Nature*. **334**:320–325.
- [43] Iyer M, Wu L, Carey M, Wang Y, Smallwood A, Gambhir SS (2001). Two-step transcriptional amplification as a method for imaging reporter gene expression using weak promoters. *Proc Natl Acad Sci USA*. **98**:14595–14600.
- [44] Zhang L, Adams JY, Billick E, Ilagan R, Iyer M, Le K, Smallwood A, Gambhir SS, Carey M, Wu L (2002). Molecular engineering of a two-step transcription amplification (TSTA) system for transgene delivery in prostate cancer. *Mol Ther*. **5**:223–232.
- [45] Huang M, Batra RK, Kogai T, Lin YQ, Hershman JM, Lichtenstein A, Sharma S, Zhu LX, Brent GA, Dubinett SM (2001). Ectopic expression of the thyroperoxidase gene augments radioiodide uptake and retention mediated by the sodium iodide symporter in non-small cell lung cancer. *Cancer Gene Ther*. **8**:612–618.
- [46] Conley BA, Egorin MJ, Sridhara R, Finley R, Hemady R, Wu S, Tait NS, Van Echo DA (1997). Phase I clinical trial of all-trans-retinoic acid with correlation of its pharmacokinetics and pharmacodynamics. *Cancer Chemother Pharmacol*. **39**:291–299.
- [47] Adamson PC (1994). Clinical and pharmacokinetic studies of all-trans-retinoic acid in pediatric patients with cancer. *Leukemia*. **8**:1813–1816.